



	<b>Experiment title:</b> Understanding the assembly of the <i>Archaeoglobus fulgidus</i> ferritin nanocage	<b>Experiment number:</b> MX-1961
<b>Beamline:</b> BM29	<b>Date of experiment:</b> from: 3 October 2017 to: 4 October 2017	<b>Date of report:</b> 11/1/2018
<b>Shifts:</b>	<b>Local contact(s):</b> Gabriele Giachin	<i>Received at ESRF:</i>
<b>Names and affiliations of applicants (* indicates experimentalists):</b> *LEVANTINO Matteo (ESRF & University of Palermo, Dept. of Physics and Chemistry) BOFFI Alberto (Sapienza University of Rome, Dept. of Biochemical Sciences & CNR- IBPM) CAMMARATA Marco (Université de Rennes 1, Institut de Physique de Rennes) *EXERTIER Cécile (Sapienza University of Rome, Dept. of Biochemical Sciences) *TRABUCO Matilde (Sapienza University of Rome, Dept. of Biochemical Sciences) MALATESTA Francesco (Sapienza University of Rome, Dept. of Biochemical Sciences)		

### Report:

We have engineered a novel chimeric ferritin by combining the structural features of the archaeal ferritin from *A. fulgidus* (AfFt) with the human receptor recognition properties of human H ferritin (HuHF). AfFt's roughly spherical structure displays an unusual tetrahedral symmetry that results in the appearance of four large triangular pores in the protein shell and a larger cavity volume. But more importantly, AfFt possesses a unique reversible association-dissociation property: unlike mammalian ferritins where disassembly is achieved by submitting the protein to a harsh pH jump, AfFt assembled state is dependent on ionic strength and/or divalent cation concentration [1]. These comparatively milder conditions put AfFt as an ideal scaffold for advanced drug-delivery systems, expanding the portfolio of molecules that can be encapsulated. On the other hand, human ferritin is recognized and internalized by the human transferrin receptor (TfR1), overexpressed in cancer cells but not in healthy tissues [2]. This innovative chimeric protein - humanized AfFt (HumAfFt) - was shown to maintain the self-assembly characteristic of AfFt while exhibiting the typical HuHF recognition by TfR1 [3].

Beamtime was requested in order to obtain small angle X-ray scattering (SAXS) patterns relevant to the investigation of the unique assembly properties of HumAfFt and AfFt. We have obtained data necessary to compare the ability to induce assembly of NaCl versus other divalent cation salts (MgCl<sub>2</sub>, CaCl<sub>2</sub>, SrCl<sub>2</sub> and BaCl<sub>2</sub>), and we have tested the ability of EDTA, a chelating agent, to reverse assembly. These data can help clarifying the role of cations in the self-assembly reaction and guide de design of future time-resolved SAXS experiments.

Beamtime began with the standard alignment and calibration procedures carried by the beamline scientist, where the scattering of the empty capillary, water and a BSA solution were evaluated.

Since we have previously collected scattering data on HumAfft, in order to confront results, data collection on the HumAfft sample was prioritized and, as time revealed insufficient to test both proteins, all the following results refer only to humAfft.

SAXS profiles were collected at increasing NaCl concentrations, spanning from 1 to 600mM (Figure 1). At intermediate salt concentrations (from 50 to 250 mM NaCl) visible protein precipitation occurred during sample preparation. Visible precipitation was removed with centrifugation and data collected for the remaining soluble fraction. Interestingly the obtained curves showed marked features, other than the expected high intensity at very low  $q$  resulting from residual aggregates. Indeed, also an intense peak at  $\sim 1 \text{ nm}^{-1}$  was observed, mixed with the underlying features of the assembled and disassembled state of humAfft, as shown in Figure 1 B. Raw images actually suggest that a fiber diffraction like pattern is actually superimposed to the solution scattering one. Formation of fibers is known to happen in protein aggregation and exploring this kind of ‘non-productive’ aggregation - meaning that a closed, spheric ferritin cage is not formed - may provide clues on the ‘productive’ mechanism of ferritin assembly.

With a preliminary data analysis during the beamtime, it became clear that titration of the radius of gyration ( $R_g$ ) with increasing NaCl, using the Guinier approximation, would not be possible and further experiments are necessary to understand this unforeseen concentration dependent aggregation.

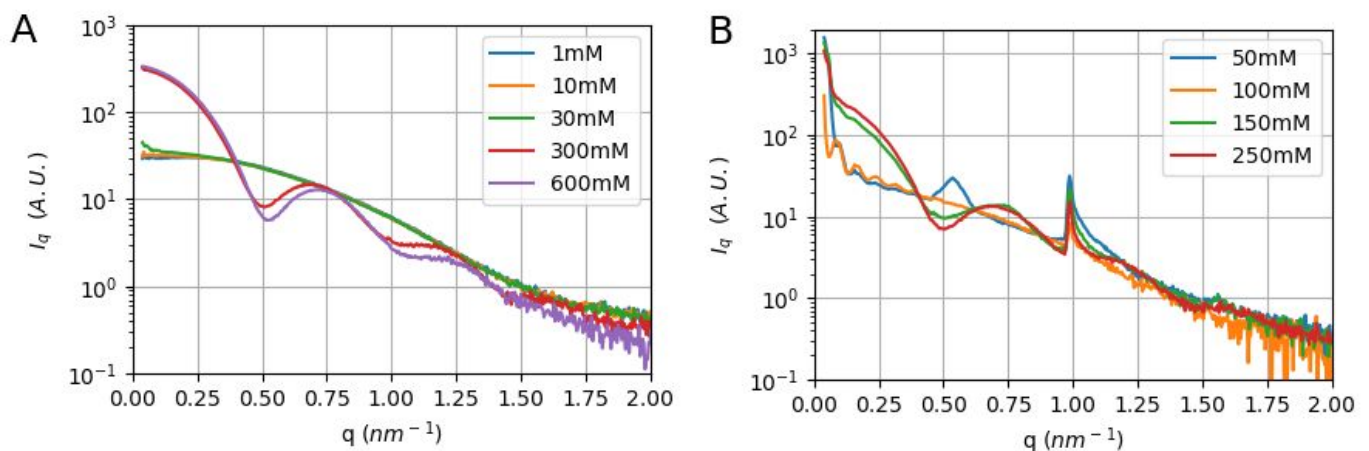


**Figure 1-** SAXS curves at increasing NaCl concentrations for samples not affected by precipitation (A) and for samples where precipitation occurred (B). Protein concentration was kept at 2.5 mg/mL for samples exempt of aggregation and for all other, protein concentration was determined before measurements and the obtained SAXS profiles normalized to it.

We proceeded to collect SAXS patterns at increasing  $\text{MgCl}_2$  concentrations. Previously collected SAXS patterns at selected  $\text{MgCl}_2$  concentrations had revealed the high cooperativity of the assembly with a sharp sigmoidal increase of the  $R_g$ . Nevertheless, a wider and finer  $\text{MgCl}_2$  concentrations range proved necessary for the fitting of possibly compatible models for the assembly mechanisms. The collected scattering curves are displayed in figure 2 A and the calculated  $R_g$  in function of  $\text{MgCl}_2$  plotted in figure 2 B.

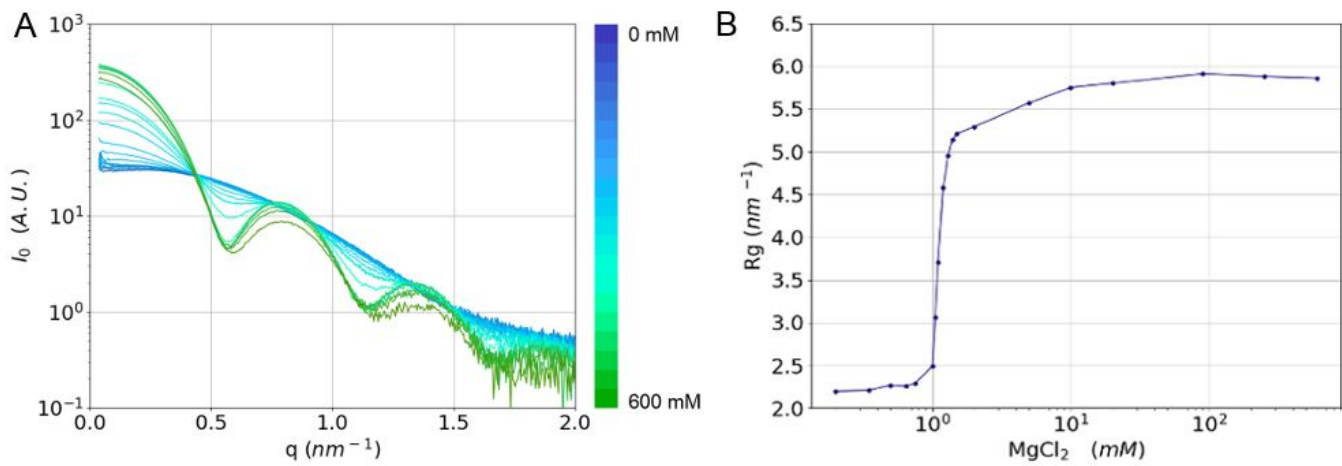


**Figure 2** - Data obtained at increasing  $\text{MgCl}_2$  concentrations with fixed 2.5 mg/mL protein concentration. (A) SAXS curves; (B) Calculated  $R_g$ .

We have then tested the ability to induce self-assembly of other divalent cations salts. Besides  $\text{MgCl}_2$  we tested  $\text{CaCl}_2$ ,  $\text{SrCl}_2$  and  $\text{BaCl}_2$ . The obtained SAXS curves are shown in figure 3 and were obtained at a fixed protein concentration of 2.5 mg/mL and 30 mM of each salt. The obtained results show a similar SAXS profile for all tested divalent cations salts, compatible with an assembled state of humAftt, and a contrasting SAXS profile for 30mM NaCl, where assembly is not attained. These findings suggest that divalent cations salts are able to induce assembly in a similar manner and that different forces govern the NaCl dependent assembly. Even at higher ionic strength, (see 100mM NaCl, see figure 2 B) NaCl is not able to promote the assembled state, revealing an added effect of divalent cations in the assembly.

From these data, another aspect stands out: the curve obtained with  $\text{CaCl}_2$ , although similar to the rest and sufficient to demonstrate assembly, shows signs of sample aggregation at low  $q$ . This was expected, since X-rays promote the formation of insoluble  $\text{CaCO}_3$  aggregates, and precludes the titration of the radius of gyration with increasing  $\text{CaCl}_2$  concentrations.

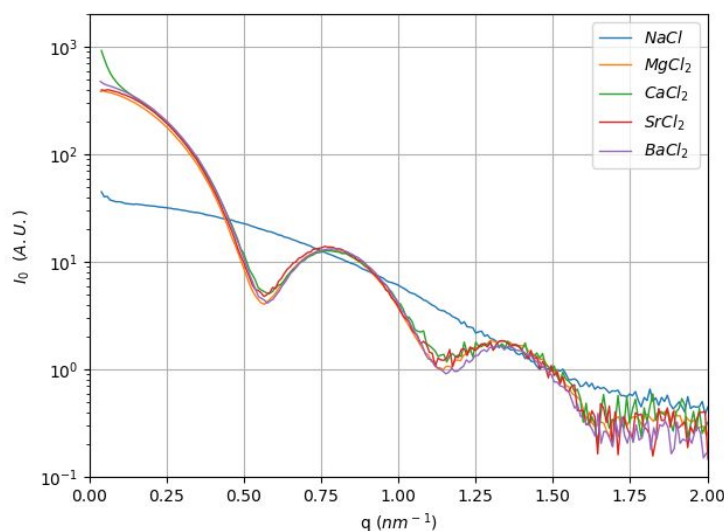


**Figure 3** - Comparison of SAXS curves using NaCl,  $\text{MgCl}_2$ ,  $\text{CaCl}_2$ ,  $\text{SrCl}_2$  and  $\text{BaCl}_2$ . Protein concentration was fixed at 2.5 mg/mL.

We have then proceeded to collecting SAXS profiles at selected  $\text{SrCl}_2$  concentrations, as to obtain a comparison on the efficiency of the different salts to induce assembly. The obtained  $R_g$  were compared to those obtained with  $\text{MgCl}_2$  and they are in good agreement, as shown in figure 4. This hints that the same forces are acting on the mechanism of assembly.

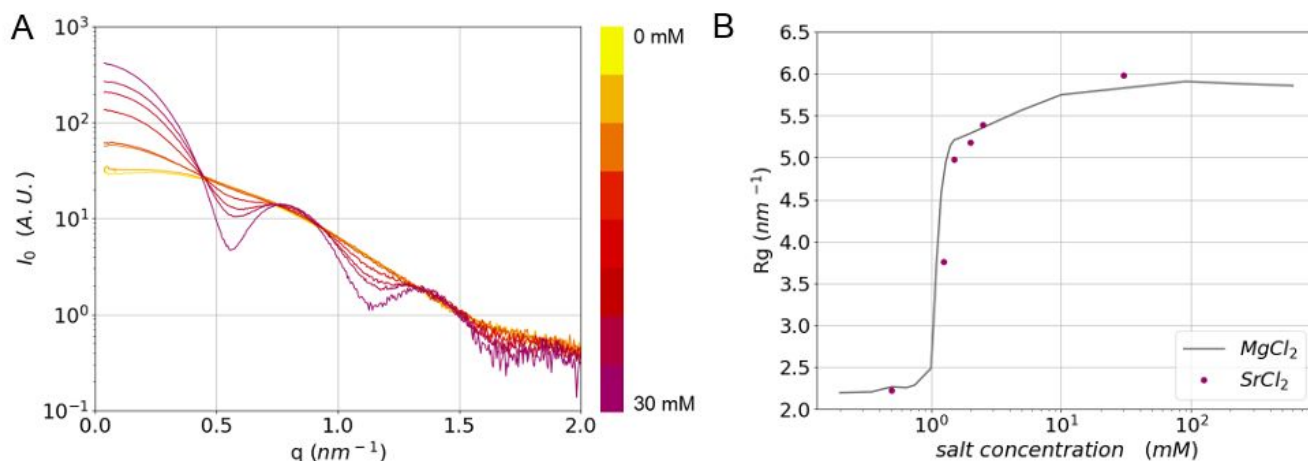


**Figure 4** - Data obtained at increasing  $\text{SrCl}_2$  concentrations and fixed 2.5 mg/mL protein concentration. (A) SAXS curves; (B) Calculated  $R_g$  plotted against increasing salt concentrations.

Lastly, we tested the ability of EDTA, a compound able to chelate  $\text{Mg}^{2+}$ , to reverse ferritin's assembly. Unexpectedly, under the tested conditions EDTA was not able to disassemble the ferritin cage (see figure 5). However, when compared to the same  $\text{MgCl}_2$  concentration, a clear change in the curve shape occurred, with the minima being less pronounced and shifted to the left. This could indicate that EDTA is indeed able to quelaete the excess  $\text{Mg}^{2+}$ , which results in a structural change, possibly an alternative cage conformation. Moreover, this has drawn our attention to the curves obtained at high NaCl concentrations (300mM, 600mM), which are also affected from flattening and minima shifts. This could imply that EDTA is able to cancel the added effect of  $\text{Mg}^{2+}$  while still able to maintain an assembled stable similar to that observed with NaCl.

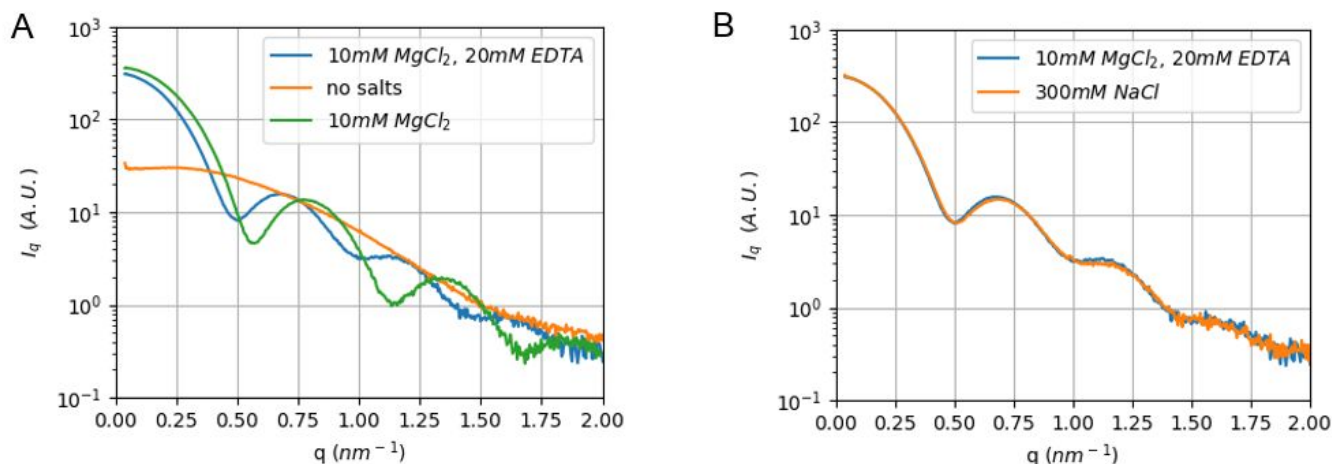


**Figure 5** - Testing the ability of  $\text{Mg}^{2+}$  chelation by EDTA to revert humAfT's assembly. Obtained SAXS profile at 1:2 ratio Mg/EDTA (10mM and 20mM, respectively) is compared to (A) the SAXS curves obtained with no salt and at 10 mM  $\text{MgCl}_2$ ; (B) the lowest NaCl concentration able to sustain assembly (300mM NaCl).

## Conclusions

From the point of view of data collection of relevant SAXS patterns for the investigation of humAfFt assembly properties, the beamtime was successful and productive. In summary, we have tested the ability of NaCl and a set of divalent cations to induce assembly, titrated the  $R_g$  at increasing  $MgCl_2$  and  $SrCl_2$  concentrations, and tested EDTA chelating effect on  $Mg^{2+}$ . Nevertheless, the available beamtime was insufficient to carry titration with  $BaCl_2$  and to explore other conditions with EDTA able to reverse assembly.

We plan to assess our data's compatibility with models proposed for the ferritin assembly mechanism, which may prove relevant for the design of new ferritin-based nanodevices. The collected data will be part of a publication currently being prepared and will also serve in the planning of future static and time-resolved SAXS experiments.

Moreover, it was not possible to carry out measurements on the wild type *A. fulgidus* ferritin which represents the reference system for all the AfFt based encapsulating systems we plan to develop and use for biotech applications.

## References:

- [1] Sana, B., Johnson, E., & Lim, S. (2015). The unique self-assembly/disassembly property of *Archaeoglobus fulgidus* ferritin and its implications on molecular release from the protein cage. *Biochimica et Biophysica Acta - General Subjects*, 1850(12), 2544–2551.
- [2] Li, L., Fang, C. J., Ryan, J. C., Niemi, E. C., Lebron, J. A., Bjorkman, P. J., ... Seaman, W. E. (2010). Binding and uptake of H-ferritin are mediated by human transferrin receptor-1. *Proceedings of the National Academy of Sciences*, 107(8), 3505–3510.
- [3] de Turrís, V., Cardoso Trabuco, M., Peruzzi, G., Boffi, A., Testi, C., Vallone, B., ... Baiocco, P. (2017). Humanized archaeal ferritin as a tool for cell targeted delivery. *Nanoscale*, 9(2), 647–655.